



Design and synthesis of the basic Cu-doped zeolite X catalyst with high activity in oxidative coupling reactions



Shengchun Chen^a, Zhen Shao^a, Zhongxue Fang^a, Qun Chen^{a,*}, Ting Tang^a, Wenqian Fu^a, Lei Zhang^a, Tiandi Tang^{a,b,*}

^a School of Petrochemical Engineering, Changzhou University, Changzhou, Jiangsu 213164, People's Republic of China

^b College of Chemistry and Materials Engineering, Wenzhou University, Wenzhou, Zhejiang 325035, People's Republic of China

ARTICLE INFO

Article history:

Received 16 December 2015

Revised 29 January 2016

Accepted 30 January 2016

Keywords:

Cu-doped zeolite X

Lewis basicity

Oxidative coupling

Cinnamic acids

ABSTRACT

The decarboxylative coupling of cinnamic acids with alcohols and the oxidative coupling of alkenes with aldehydes are typical organic reactions. Considering the characteristics and mechanisms of the reactions, the Cu-doped zeolite-X catalyst (Cu-X) with Lewis basic sites was synthesized and used for the two reactions. Compared with Cu, Cu₂O, and CuBr₂ catalysts (4–21%), the Cu-X catalyst (99%) shows extraordinary high activity in the decarboxylative coupling of cinnamic acids with alcohols. In addition, the Cu-X catalyst presents excellent performance in the oxidative coupling of alkenes with aldehydes. The strong interaction between Cu⁺ and the zeolite framework benefits the transformation of Cu²⁺ and Cu⁺ in the redox process, enhancing the reaction activity. More importantly, the Lewis basic sites on the Cu-X catalyst could favor the adsorption of the cinnamic acid, resulting in electron-rich density in the C=C bond, and therefore greatly improving the reaction activity.

© 2016 Elsevier Inc. All rights reserved.

1. Introduction

Developing highly efficient heterogeneous catalysts is of great importance in organic chemistry with a view to practical applications [1–7]. Up to now, endeavors to realize heterogeneous catalysis have been made for many important reactions, such as Heck, Suzuki, and Ullmann couplings [8–11]. Thus, significant positive information crossing from homogeneous to the heterogeneous catalysis has been achieved [12–17]. Nevertheless, the structure, properties, and stability of the active centers in heterogeneous catalysts are difficult to control in a flexible way to meet the demands of reaction activity and selectivity. Modern synthetic chemistry especially tends to be more complicated [18–22], seeking to design more elaborate catalytic active centers. Therefore, it must consider the reaction characteristics, reaction mechanisms, and even the structure and nature of the reactant molecules, and should combine the support properties to rationally construct the active centers in heterogeneous catalysts.

As an example, the decarboxylative coupling of cinnamic acids with alcohols is a useful route for the synthesis of allyl alcohol derivatives [23–25], which are important intermediates for the preparation of pharmaceuticals and organic materials [26,27]. From Fig. 1, cinnamic acid (CA) coordinates with Cu²⁺ species to form a complex [28]. Subsequently, the C=C bond in the complex is attacked by the α -carbon-centered radical, forming an active intermediate that transforms to allyl alcohol by reductive elimination, accompanying the formation of CO₂ and the transformation of Cu²⁺ to Cu⁺ [29]. Therefore, in this process, the activation of the C=C bond in the CA molecule is a key step.

In principle, enhancing the electron density of the C=C bond of the Cu-coordinated complex could enhance the electrophilic attacks of α -carbon-centered radicals (Fig. 1), which would result in an increase in reaction activity. Notably, the Lewis basic site is an electron donor; thus the catalyst with Lewis basicity should favor the adsorption of CA as well as enhancing the electron density in the C=C bond. Therefore, developing a porous heterogeneous catalyst with both Lewis basic and metal sites could greatly promote reaction activity.

Associated studies have revealed that the crystalline aluminosilicate zeolite X with three-dimensional large pore structure benefits reactant molecule diffusion [30,31]. In especial, the negatively charged frameworks with low Si/Al ratios (<1.5) endow zeolite X with relatively strong Lewis basicity [32–34]. Thus, it is a

* Corresponding authors at: School of Petrochemical Engineering, Changzhou University, Changzhou, Jiangsu 213164, People's Republic of China, College of Chemistry and Materials Engineering, Wenzhou University, Wenzhou, Zhejiang 325035, People's Republic of China (T. Tang).

E-mail addresses: chenqunju@yahoo.com (Q. Chen), tangtiandi@wzu.edu.cn (T. Tang).

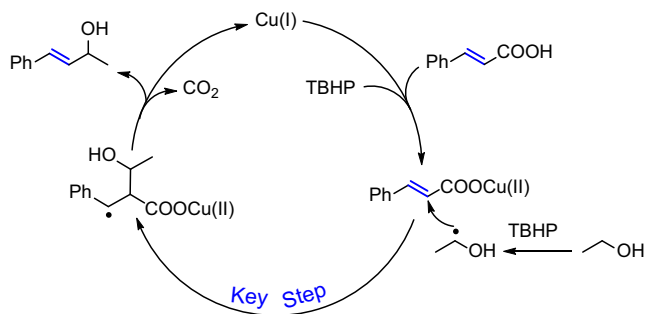


Fig. 1. Mechanism of decarboxylative coupling of CA with ethanol.

reasonable goal to synthesize transition metal-doped zeolite X with Lewis basic and metal sites for decarboxylative coupling of CAs with alcohols, alkylbenzenes, cycloalkanes, and cyclic ethers.

Here, we synthesized Cu-doped zeolite X (Cu-X) and envisioned its use to catalyze the decarboxylative coupling reaction in high activity. For comparison, Cu-doped zeolite Y (Cu-Y) and mesoporous ZSM-5 (Cu-MZSM-5) were also prepared. Compared with the Cu, Cu₂O, and CuBr₂ catalysts reported in the literature [29], the Cu-Y, Cu-MZSM-5, and especially the Cu-X catalysts show extraordinarily high activity at very low Cu content (the mole ratio of the substrate to Cu is 336:1). This should be attributed to the fact that the Cu-X catalyst not only possesses active Cu⁺ and Cu²⁺ sites but also provides abundant Lewis basic sites. The strong interaction between Cu species and the zeolite framework benefits the transformation of Cu²⁺ and Cu⁺ in the reaction, and the Lewis basic sites as electron donors enhance the electron density of the C=C bond in the CA molecule, which greatly facilitates the C=C bond radical addition with electrophilic α -carbon-centered radicals. Furthermore, this catalyst design concept was also applied to synthesize Fe-, Co-, and Ni-doped zeolite X as highly active catalysts for the preparation of very useful α,β -epoxy ketone compounds via direct oxidative coupling of alkenes with aldehydes.

2. Experimental

2.1. Materials synthesis

Cu-containing zeolite X (Cu-X) was prepared from a starting aluminosilicate gel with molar ratio 1 Al₂O₃/3.5 Na₂O/3 SiO₂/0.08 CuO/186 H₂O. In a typical run, water glass (9.9 mL) was mixed with an aqueous solution (25.4 mL, 7.7 wt.%) of NaOH under vigorous stirring for 1 h. Then the aqueous solution (27.0 mL, 11.8 wt.%) of NaAlO₂ was added and further stirred for 1 h at room temperature. After that, the reaction mixture was stirred at 75 °C for another 4 h. Finally, an aqueous solution (2.0 mL, 0.3467 g) of Cu(NO₃)₂·3H₂O was added dropwise and stirred for 1 h to yield an aluminosilicate gel. The gel was transferred into a Teflon-coated stainless steel autoclave for static crystallization at 100 °C for 84 h. After filtration and washing, the sample was dried overnight at 120 °C and calcined in air at 550 °C. Fe-, Co-, and Ni-containing zeolite X (Fe-X, Co-X, and Ni-X) were also synthesized in similar procedures by the addition of Fe₂(NO₃)₃·9H₂O (0.6693 g), Co(NO₃)₂·6H₂O (0.456 g), and Ni(NO₃)₂·6H₂O (0.4622 g), respectively.

Cu-containing zeolite Y (Cu-Y) was prepared from a starting aluminosilicate gel with molar ratio 1 Al₂O₃/4 Na₂O/9 SiO₂/0.32 CuO/170 H₂O. In a typical preparation, water glass (19.4 mL), H₂O (3.6 mL), and a solution (3.4 mL) of zeolite Y seed (prepared by mixing NaAlO₂ (1.409 g), H₂O (18.1 mL), NaOH (5.0776 g), and water glass (17.3 mL), followed by aging at room temperature for 24–36 h) were mixed. After 30 min of stirring at room temperature, an aqueous solution (2.0 mL, 0.3467 g) of Cu(NO₃)₂·3H₂O was added dropwise and further stirred for 1 h. After that, an aque-

ous solution (5.7 mL, 23.4 wt.%) of Al₂(SO₄)₃ and an aqueous solution (5.95 mL, 18.2 wt.%) of NaAlO₂ and NaOH (9.2 wt.%) were added. The mixture was stirred at room temperature for 60 min, producing a viscous aluminosilicate gel. The gel was transferred into a Teflon-coated stainless steel autoclave for crystallization at 100 °C for 24 h. After filtration and washing, the sample was dried overnight at 120 °C and calcined in air at 550 °C.

The Cu-containing mesoporous zeolite ZSM-5 (Cu-MZSM-5) was synthesized using silane of N,N-dimethyl-N-octadecyl-N-(3-triethoxysilylpropyl)ammonium bromide (TPOAB) as a mesoscale template according to our previous work [35]. The molar ratio of various compositions was 1 Al₂O₃/1 Na₂O/2.5 CuO/69 SiO₂/15.1 TPAOH/13.2 TPOAB/1552 H₂O. Typically, NaAlO₂ (0.16 g) was dissolved in water (18.0 mL), followed by addition of tetrapropylammonium hydroxide (TPAOH, 12.0 mL) and tetraethyl orthosilicate (TEOS, 15.0 mL). After the mixture was stirred at room temperature for 4.5 h, Cu(NO₃)₂·3H₂O (0.6 g) was then introduced and the reaction mixture was stirred at 75 °C for another 5 h. Finally, TPOAB (7.5 mL) was added dropwise and stirred for 1 h to yield an aluminosilicate gel. The gel was transferred into a Teflon-coated stainless steel autoclave for static crystallization at 180 °C for 72 h. The resultant product was filtered, washed, dried overnight at 120 °C, and calcined in air at 550 °C for 5 h.

Y and MZSM-5 were exchanged with 1 M NH₄NO₃ solution at 80 °C for 4 h. After filtration, the samples were dried overnight at 120 °C and calcined at 500 °C for 4 h, transforming to acidic H-form zeolite Y (HY) and H-form zeolite MZSM-5 (HMZSM-5).

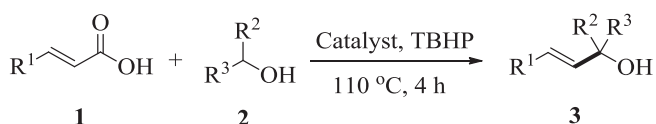
2.2. Characterization

The X-ray powder diffraction (XRD) pattern was recorded on a D/MAX 2500/PC powder diffractometer (Rigaku) using a Cu K α radiation source operated at 40 kV and 200 mA. Nitrogen physisorption was conducted at –196 °C on a Micromeritics ASAP 2020M apparatus. The sample was degassed at 300 °C for 8 h before the measurement. Specific surface area was calculated from the adsorption data using the Brunauer–Emmett–Teller (BET) equation. The Cu content and the Si/Al ratios were determined by inductively coupled plasma optical emission spectroscopy (ICP-OES) with a Perkin-Elmer 3300DV emission spectrometer. The transmission electron microscopy (TEM) image was obtained on a JEM-2100F microscope with a limited line resolution capacity of 1.4 Å at 200 kV. Before characterization by TEM, the sample was cut into thin slices and dropped onto a Ni grid coated with a carbon membrane. X-ray photoelectron spectroscopy (XPS) experiments were performed on an ESCALAB MK II system. The basicity of the zeolite samples was measured on a Bruker TENSOR 27 infrared spectroscopy (IR) equipped with a reactor cell. Before being dosed with pyrrole, the sample was outgassed overnight at 400 °C and 10^{–3} Pa. After cooling to room temperature, the sample was exposed to pyrrole vapor until saturated, followed by evacuation at 65 °C for 60 min. The spectrum was recorded at 65 °C with a 2 cm^{–1} resolution and using a 32-scan spectrum. The UV–vis diffuse reflectance (UV–vis) spectrum was obtained on a Perkin-Elmer Lambda 25 spectrometer with an integration sphere. The IR spectrum of the CA-chemisorbed Cu-X (Cu-X-CA) sample was obtained on a Bruker TENSOR 27 infrared spectroscopy equipped with a reactor cell. Before measurement, the Cu-X-CA sample was evacuated to 10^{–3} Pa at 100 °C for 20 h, and then the temperature was increased to 110 °C. The spectrum was obtained in the absorbance mode and was shown after subtraction of a background spectrum obtained on the Cu-X sample. For comparison, the IR spectrum of CA was also recorded at room temperature. The ¹³C solid-state NMR spectra of Cu-X-CA and CA were obtained on a Bruker AVANCE III 400WB spectrometer operated at 9.4 T with a frequency of 100.62 MHz. The Cu-X-CA sample was pre-outgassed overnight at 100 °C and 10^{–1} Pa and then packed into a 4 mm zirco-

nia rotor. The contact time was 1.5 ms, and the recycle delay was 0.5 s for Cu-X-CA and 60 s for CA, respectively, which were adjusted to three times $^1\text{H} T_1$ values. A ramp-contact and spinal 64 decoupling pulse program was used. The numbers of scans of ^{13}C CP-MAS were 156,000 for Cu-X-CA and 16 for CA, with rotor spinning rates of 14 kHz. The spectra were calibrated using the methine carbon atoms of adamantane as an external standard ($\delta = 29.47$ ppm).

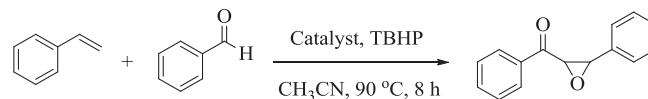
2.3. Activity test

The typical experimental procedure for the decarboxylative coupling reaction was as follows: Cu-X catalyst (5 mg), CA 1 (0.5 mmol), TBHP (1.0 mmol, 70% aqueous solution), and ethanol 2 (2.0 mL) were placed in a sealed tube (10 mL). The reaction was heated at 110 °C for 4 h. After the reaction finished, the catalyst was separated by centrifugation and filtration to obtain the liquid phase. The liquid products were analyzed by an Agilent 1260 Infinity Liquid Chromatogram. The pure product was obtained by flash column chromatography on silica gel using petroleum ether (60–90 °C) and ethyl acetate as eluents. Compounds described in the literature were characterized by comparing their ^1H and ^{13}C NMR spectra and MS data with the reported data. The ^1H NMR (500 and 400 MHz) and ^{13}C NMR (125 and 100 MHz) were recorded with spectrometers at 20 °C using CDCl_3 as the solvent. Chemical shifts are given in parts per million relative to TMS as the internal standard at room temperature:



The typical experimental procedure for synthesis of α,β -epoxy ketones: catalyst (40 mg) was added to a Schlenk tube equipped

with a magnetic stirrer bar. Styrene (0.5 mmol), benzaldehyde (2 equiv, 1.0 mmol), TBHP (1.0 mmol, 70% aqueous solution), and acetonitrile (2.0 mL) as a solvent were injected into the reaction tube. The reaction mixture was then heated to 90 °C and stirred for 8 h. Once the reaction was finished, the catalyst was separated by centrifugation and filtration to obtain the liquid phase. The liquid products were analyzed with an Agilent 1260 Infinity Liquid Chromatogram. The pure product was obtained by flash column chromatography on silica gel (petroleum ether/ethyl acetate = 50:1):



2.4. Cinnamic acid adsorption experiment

The typical adsorption experimental procedure was carried out in a 25 mL sealed tube with a magnetic stirrer bar. The CA (14 mg) was dissolved in cyclohexane (10 mL), and then 1.0 g catalyst was added. The mixture was heated at 110 °C for 6 h under stirring. After cooling to room temperature, the liquid phase was analyzed with an Agilent 1260 Infinity Liquid Chromatogram. The solid sample was washed with cyclohexane (15 mL) 20 times and dried at 60 °C for 48 h. The solid sample was used for characterization of UV-vis DRS, IR, and solid state NMR.

3. Result and discussion

3.1. General properties of the catalysts

The XRD patterns in Fig. 2a reveal that the Cu-X sample has well-resolved peaks in the range 4–50° with faujasite structure. Although the crystalline phases of Cu species are not detected,

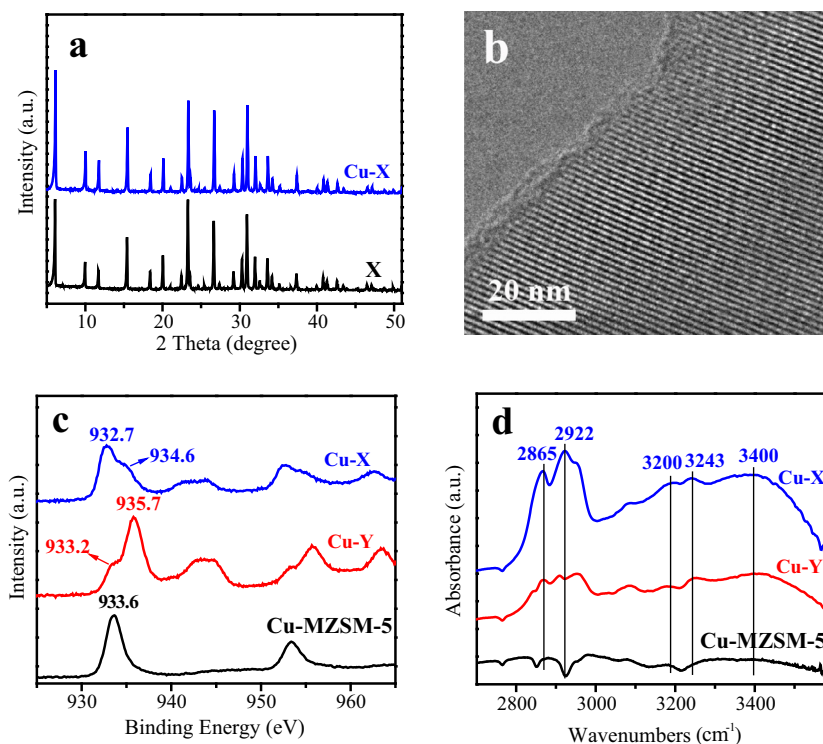


Fig. 2. (a) XRD patterns of Cu-X and X zeolites, (b) TEM image of Cu-X zeolite, (c) XPS spectra of Cu-X, Cu-Y, and Cu-MZSM-5 zeolites, and (d) IR spectra of pyrrole-adsorbed Cu-X, Cu-Y, and Cu-MZSM-5 samples.

the Cu content in the Cu-X sample is 1.9 wt.%, determined by inductively coupled plasma analysis, suggesting that the Cu species are highly dispersed in the zeolite X structure. The TEM images of the thin sectioned samples show that Cu-X has a highly crystalline micropore structure and the Cu particles cannot be observed (Fig. 2b and Fig. S1 in the Supplementary Information). However, the energy-dispersive X-ray spectroscopy point analysis confirms the presence of Cu (0.54 wt.%) in the selected zone (Fig. S2 in the Supplementary Information), further suggesting that the Cu species are well confined in the micropore structure of the Cu-X catalyst. Sample textual parameters are presented in Table 1.

The electron states of the Cu species in the Cu-X, Cu-Y, and Cu-MZSM-5 samples were analyzed by X-ray photoelectron spectroscopy (XPS) (Fig. 2c). The binding energy of $\text{Cu}2p_{3/2}$ at 932.7 and 934.6 eV for the Cu-X sample is assigned to the characteristics of the Cu^+ and Cu^{2+} species, respectively [36,37]. The binding energy of $\text{Cu}2p_{3/2}$ at 933.2 and 933.6 eV for the Cu-Y and Cu-MZSM-5 catalysts is assigned to the characteristics of the $\text{Cu}^{\delta+}$ ($\delta < 2$) species (Fig. 2c) [36,37]. The presence of the Cu^+ and $\text{Cu}^{\delta+}$ species in Cu-X, as well as Cu-Y and Cu-MZSM-5, could be attributed to the strong interaction of Cu species with the zeolite framework [38], resulting in electron transfer from the framework oxygen to the Cu species. The UV-vis spectra of the Cu-X, Cu-Y, and Cu-MZSM-5 samples in Fig. S3 in the Supplementary Information also show a broad absorption band at 230–320 nm associated with Cu^+ and Cu^{2+} [35,39].

Table 1
Texture parameters of all samples.

Sample	S_{BET} (m^2/g) ^a	S_{ext} (m^2/g) ^b	V_{mic} (cm^3/g) ^c	V_{meso} (cm^3/g) ^d	Si/Al
X	814	27	0.32	0.01	1.2
Cu-X	772	39	0.29	0.03	1.3
Cu-Y	825	72	0.30	0.08	2.6
Cu-MZSM-5	516	273	0.10	0.32	40.5

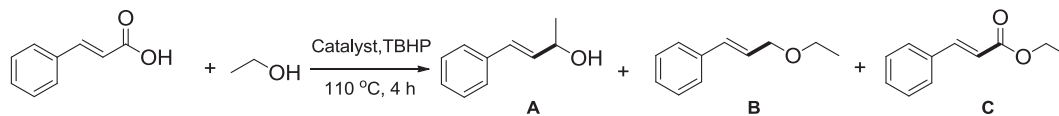
^a BET surface area.

^b External surface area.

^c Microporous pore volume.

^d Mesoporous pore volume.

Table 2
Decarboxylative coupling of CA with ethanol over different catalysts.^a



Entry	Catalyst	Cu content (μmol) ^b	Conversion (%) ^c	Selectivity (%)		
				A	B	C
1	X ^d	–	44	~100	–	–
2	Y ^d	–	27	92	8	–
3	MZSM-5 ^d	–	18	78	22	–
4	HY ^d	–	69	15	70	15
5	HMZSM-5 ^d	–	72	13	72	15
6	Cu-X ^d	1.48	99	~100	–	–
7	Cu-Y ^d	1.64	62	~100	–	–
8	Cu-MZSM-5 ^d	1.4	43	96	–	–
9	Cu	10	21	~100	–	–
10	Cu_2O	20	8	~100	–	–
11	CuBr_2	10	4	~100	–	–

^a Reaction conditions: CA (0.5 mmol), ethanol (2.0 mL), and TBHP (1.0 mmol).

^b Cu content in the reaction system.

^c Cinnamic acid conversion by LC analysis.

^d Zeolite catalyst of 5 mg.

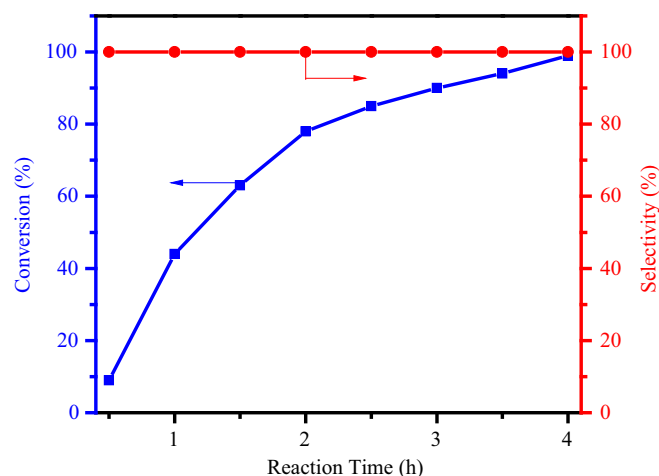


Fig. 3. Dependence of the CA conversion and product selectivity on reaction time over Cu-X catalyst (5 mg catalyst, 0.5 mmol CA, 1.0 mmol TBHP, 2.0 mL ethanol, reaction temperature 110 °C).

Table 3
Effect of the metal content in the Cu-X and Cu-Y catalysts on catalytic activity in the decarboxylative coupling of CA with ethanol.^a

Catalyst	Copper content (wt.%)	Conversion (%) ^b	Selectivity (%)
Cu-X ^c	0.8	75	100
	1.2	85	100
	1.9	88	100
	2.3	87	100
Cu-Y ^d	0.7	51	100
	1.1	67	100
	2.1	62	100
	2.4	64	100

^a Reaction conditions: CA (0.5 mmol), ethanol (2.0 mL), catalyst (5 mg), TBHP (1.0 mmol), at 110 °C.

^b Conversion of CA by LC analysis.

^c Reaction time is 3 h.

^d Reaction time is 4 h.

To characterize the basicity of the catalysts, the pyrrole-adsorbed catalyst sample was studied by in situ infrared spectroscopy (IR). As shown in Fig. 2d, the characteristic peaks of NH stretching at 3400, 3243, and 3200 cm^{-1} , combined with the bands at about 2922 and 2865 cm^{-1} , reveal the basic sites on the surfaces of the Cu-X and Cu-Y samples [40]. However, the intensities of the absorption peaks on the Cu-X sample are much stronger than on the Cu-Y sample, which indicates that the basicity of the Cu-X cat-

alyst is stronger than that of the Cu-Y catalyst. The Cu-MZSM-5 catalyst has almost no basicity.

3.2. Catalyst performance

Table 2 gives the decarboxylative coupling of CA with ethanol over a series of catalysts. Obviously, the basic zeolite X gives a moderate CA conversion of 44% and high target product selectivity (100%), much higher than zeolite Y and MZSM-5 (entries 1–3). Notably, the conversion of CA over acidic HY and HMZSM-5 is higher than over the corresponding Y and MZSM-5 and X catalyst; however, a large amount of byproducts is formed due to esterification and etherification reactions (entries 4, 5). These results indicate that the zeolite X catalyst with basicity can inhibit the occurrence of side reactions. When the Cu was introduced into the zeolites, the activity of the catalysts was increased (entries 6–8). In addition, although the Cu content in the reaction systems with Cu-X, Cu-Y, and Cu-MZSM-5 catalysts (1.4–1.64 μmol) is much less than that in the Cu, Cu_2O , and CuBr_2 catalysts (10–20 μmol), the activity of the Cu-X (99%), Cu-Y (62%), and Cu-MZSM-5 (43%) catalysts is much higher than that of those catalysts (4–21%, entries 6–11). The conversion of the CA with reaction time over the Cu-X catalyst is shown in Fig. 3. The product selectivity is close to 100% under all conversions. In addition, the reaction activity increased with increased concentration of ethanol and the oxidant (TBHP) (Tables S1 and S2 in the Supplementary Information). Table 3 gives the activity of the Cu-X and Cu-Y catalysts with different Cu content. Clearly, the conversion of CA over Cu-X and Cu-Y catalysts is not obviously increased with Cu content in the range 1.2–2.3 wt.% for Cu-X and 1.1–2.4 wt.% for Cu-Y catalysts.

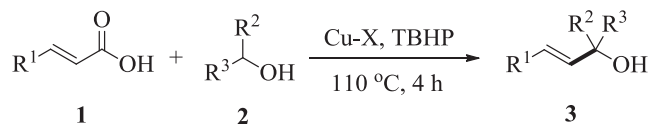
Table 4
Decarboxylative coupling of CA with alkylbenzenes, cycloalkanes, and cyclic ethers.^a

Substrate 1	Substrate 2	Product	Conversion (%) ^b
	Toluene		83 (60, 41)
	<i>m</i> -Xylene		89 (54, 35)
	Cyclohexane		90 (49, 32)
	Cyclooctane		75 (38, 18)
	1,4-Dioxane		86 (41, 15)
	Tetrahydrofuran		94 (38, 17)

^a Reaction conditions: substrate 1 (0.5 mmol), substrate 2 (2.0 mL), Cu-X, Cu-Y, and Cu-MZSM-5 catalysts (5 mg), TBHP (1.0 mmol), at 110 °C for 4 h.

^b The conversions in parentheses are obtained over Cu-Y and Cu-MZSM-5 catalysts (for all the reactions, the selectivity is 100%).

Table 5
Decarboxylative coupling of vinyl acids with alcohols.^{a,b}



Entry	Vinyl acids	Alcohols	Product 3	Yield (%)
1		Ethanol		99
2		Isopropanol		90
3		Methanol		94
4		<i>n</i> -Butanol		83
5		Cyclohexanol		85
6		Ethanol		86
7				91
8				84

^a Conversion of the vinyl acids by LC analysis.

^b Selectivity is 100%. Reaction conditions: vinyl acid substrate (0.5 mmol), alcohol substrate (2.0 mL), Cu-X (5 mg), TBHP (1.0 mmol), at 110 °C for 4 h.

However, when the Cu content in the Cu-X and Cu-Y catalysts was decreased to 0.8 and 0.7 wt.%, respectively, the conversion of CA over Cu-X and Cu-Y catalysts was reduced.

To further investigate the activity of the Cu-X catalyst on the other substrates with different natures, the decarboxylative coupling of CA with various compounds such as alkylbenzenes, cycloalkanes, and cyclic ethers was tested (Table 4). The results show that the activity of the Cu-X catalyst is higher than that of Cu-Y and Cu-MZSM-5 catalysts.

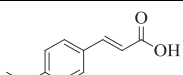
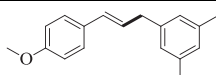
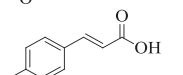
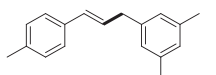
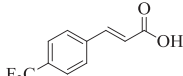
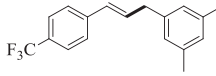
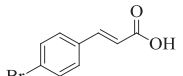
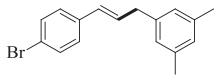
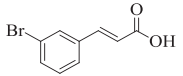
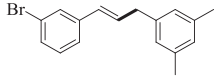
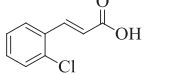
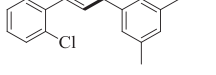
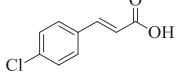
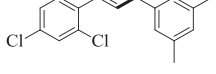
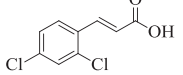
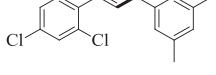
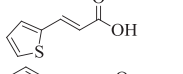
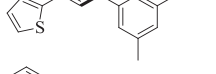
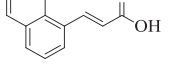
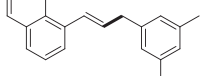
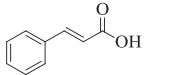
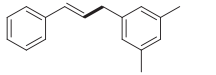
The generality of the Cu-X catalyst was further investigated in the decarboxylative coupling of CAs with a series of alcohols (Table 5). Obviously, the decarboxylative cross-coupling reaction over Cu-X catalyst shows broad tolerance for various primary and secondary alcohols. All selected alcohols reacted with CA, affording the corresponding allylic alcohols 3a–3e in good to high yield (83–99%). The Cu-X catalyst also shows high activity when the CA with electron-deficient groups is selected as substrate, giving the desired products 3f–3h in 84–91% yield. In addition, the Cu-X catalyst was used in the coupling reaction of CAs (containing electron-withdrawing or electron-donating groups) with mesitylene, affording the corresponding products in good yield (entries 1–8, Table 6). Furthermore, the Cu-X catalyst also presents excellent catalytic performance in the decarboxylative coupling of vinyl acids (containing 2-thienyl or 1-naphthyl) with mesitylene (entries 9 and 10, Table 6).

3.3. Discussion of high reaction activity

The extraordinarily high activity and broad scope of reactants over the Cu-X catalyst should be attributed to the highly dispersed Cu^+ and Cu^{2+} species, and especially the relatively strong Lewis basic sites on zeolite X. From Fig. 1, in the decarboxylative coupling of the CA with ethanol, the transformation of the Cu^{2+} and Cu^+ species is required. In the case of Cu-X, Cu-Y, and Cu-MZSM-5 catalysts, the strong interaction of the Cu species with the negatively charged framework could benefit the reversible transformation of the Cu^{2+} and Cu^+ species under redox conditions, facilitating the reaction activity. In contrast, such transformations are disadvantageous in the Cu, Cu_2O , and CuBr_2 catalyst systems.

More importantly, the relatively strong Lewis basic sites on zeolite X play a critical role in the improvement of the activity of the Cu-X catalyst. As mentioned above, the activation of the $\text{C}=\text{C}$ bond in the CA is a key step, and the electron-rich density in the $\text{C}=\text{C}$ bond could benefit the attack by the α -carbon-centered radical (Fig. 1). Compared with Cu-Y and Cu-MZSM-5 catalysts, the relatively strong Lewis basic sites on the Cu-X catalyst could favor the adsorption of the CA and enhance the electron density of the $\text{C}=\text{C}$ bond in the CA (Fig. 4), and thus greatly improve the reaction activity. This suggestion is strongly supported by the CA adsorption experiments and the UV–vis, IR, and NMR analyses of the CA-adsorbed Cu-X sample. Table 7 shows that the adsorption capacity (8.6–10.4 mg/g_{Cat}) of Cu-X with different Cu content is much

Table 6
Decarboxylative coupling of vinyl acids with mesitylene.^{a,b}

Entry	Substrate 1	Substrate 2	Product 4	Time (h)	Yield (%)
1				4h	92
2				4i	75
3				4j	54
4				4k	83
5				4l	62
6				4m	77
7				4n	96
8				4o	82
9				4p	65
10				4q	91
11				4r	98

^a Conversion of the vinyl acids by LC analysis.

^b Selectivity is 100%. Reaction conditions: vinyl acid substrate (0.5 mmol), mesitylene substrate (2.0 mL), Cu-X (5 mg), TBHP (1.0 mmol), at 110 °C for 4 h.

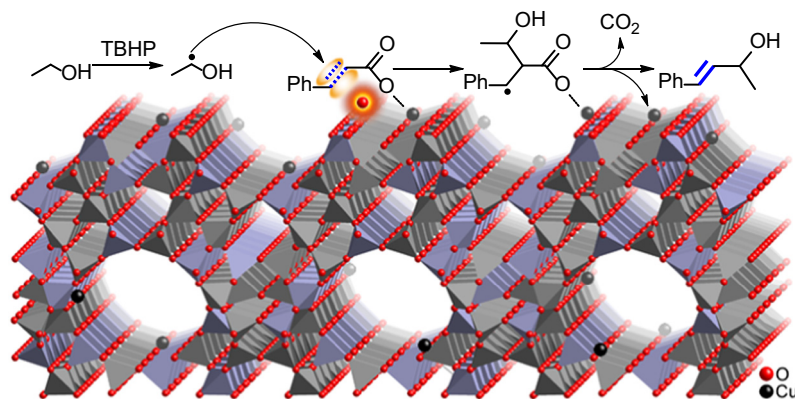


Fig. 4. Enhancement of the activity of the decarboxylation of CA with ethanol over Cu-X catalyst.

Table 7

The adsorption capacity of Cu-X, Cu-Y, and Cu-MZSM-5 catalysts for CA.

Catalyst	Copper-content (wt.%)	Adsorption capacity (mg/g _{Cat.})
Cu-X	2.3	10.4
	1.9	9.4
	1.2	8.6
X	–	5.5
Cu-Y	2.1	3.1
Cu-MZSM-5	1.8	0.9

higher than that of Cu-Y and Cu-MZSM-5 (3.1 and 0.9 mg/g_{Cat.}), confirming that the strong Lewis basic sites on the Cu-X catalyst are more favorable for the adsorption of CA molecules.

Notably, the UV-vis, IR, and NMR spectra of the CA-chemisorbed Cu-X sample (Cu-X-CA) give more important information (Figs. 5 and 6). The pure CA presents an absorption band at 270.2 nm assigned to the characteristics of the conjugated π bond in the CA molecule (Fig. 5a). After the Cu-X catalyst adsorbed the CA, this absorption band was shifted to 277.6 nm. Electron transfer from the Lewis basic sites on the Cu-X to the conjugated π bond of the adsorbed CA may have occurred, resulting in enhancement of the electron density in the C=C bond. This suggestion is also supported by IR analysis of the Cu-X-CA sample (Fig. 5b). The absence of the band at 1703 cm^{-1} for the free CA molecule is evidence of the complete deprotonation of carboxyl groups, which could be attributed to the coordination of the carboxylate oxygen atoms with the Cu species on the Cu-X catalyst. As a result, the absorption bands at 1435 and 1611 cm^{-1} associated with asymmetric and symmetric stretching vibrations of carboxylate are found in the Cu-X-CA sample. In addition, the red shift for the C=C stretching vibrations appears in the range 1450–1586 cm^{-1} in the Cu-X-CA sample, in contrast with that of the CA molecule. This phenomenon should be due to the increase of electronic density of the π -conjugated system caused by electron transfer from the Lewis basic sites on the Cu-X catalyst to the conjugated C=C bond of the adsorbed CA. These results are consistent with the result of the UV-vis determination.

In addition, the ^{13}C NMR spectra of Cu-X-CA and CA show that the characteristic peak of the carboxyl carbon in CA at 172.9 ppm shifts to 176.6 ppm after the CA are chemisorbed onto Cu-X (Fig. 6), which could be due to decreased electron density in the carboxyl carbon. This phenomenon should be caused by the coordination of carboxylate with the Cu species on the Cu-X-CA catalyst. Moreover, the two peaks at 146.7 and 119.2 ppm are characteristic of the C=C carbons in CA. The corresponding peaks are not found at relatively low field for the Cu-X-CA sample, while two peaks appear at high field at 28.7 and 21.7 ppm. It should be

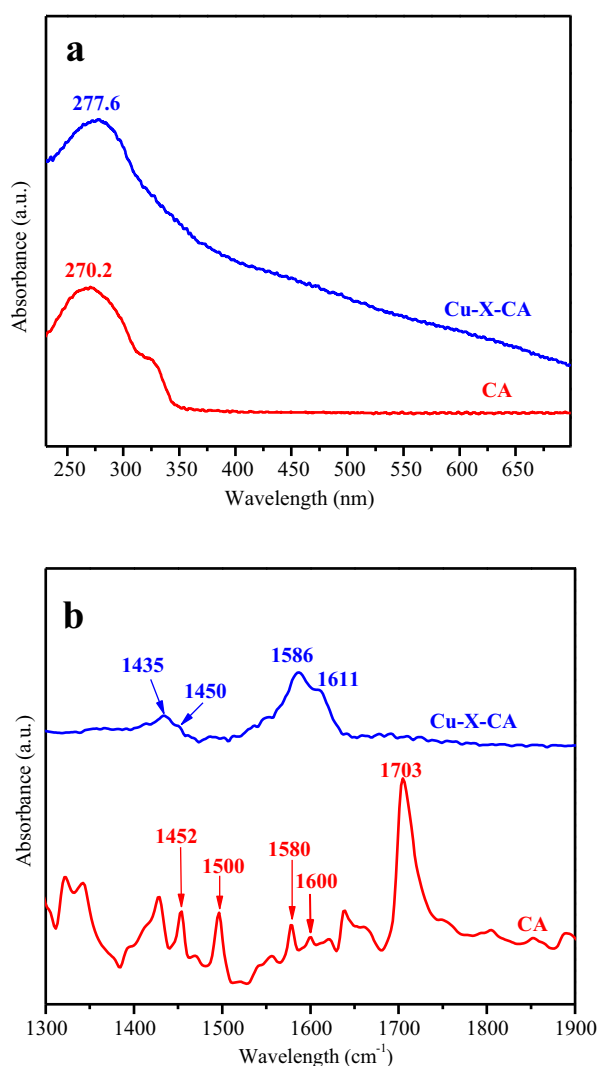


Fig. 5. (a) UV-vis and (b) IR spectra of the CA and Cu-X-CA samples.

noted that the two peaks at high field distinguished from the normal $\text{C}(sp^3)\text{--C}(sp^3)$ singles, which might be ascribed to the transition state carbons between $\text{C}(sp^2)\text{--C}(sp^2)$ double and $\text{C}(sp^3)\text{--C}(sp^3)$ bonds. As a result, the C=C bond in the CA is highly activated after the CA is chemisorbed on the Cu-X catalyst.

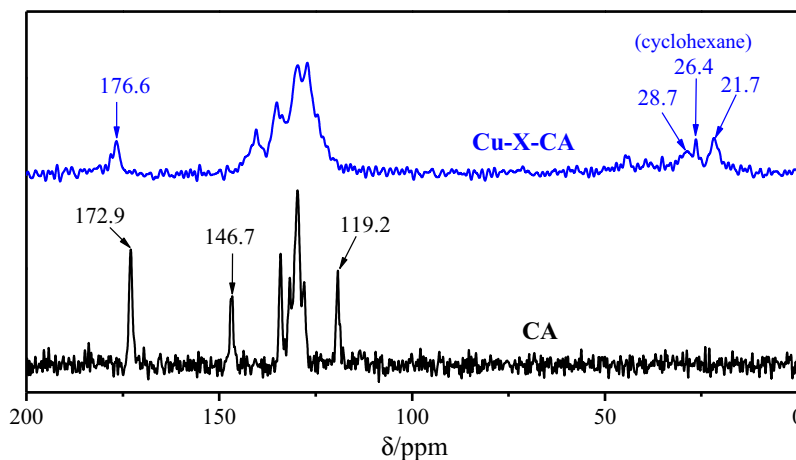
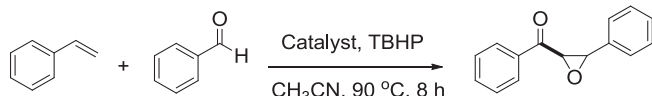


Fig. 6. The ^{13}C NMR spectra of CA and Cu-X-CA samples (the chemical shift at 26.4 ppm is caused by the carbon from the rudimentary cyclohexane).

Table 8

The oxidative coupling of styrene with benzaldehyde over series zeolite catalysts.^a



Entry	Catalyst	Conversion (%) ^b	Selectivity (%) ^c
1	X	65	93
2	Cu-X	86	87
3	Ni-X	100	93
4	Fe-X	94	89
5	Co-X	96	94

^a Reaction conditions: styrene (0.5 mmol), benzaldehyde (1.0 mmol), TBHP (1.0 mmol), catalyst (40 mg), CH_3CN (2.0 mL).

^b Conversion of the styrene is obtained by LC analysis.

^c Selectivity of the α,β -epoxy ketone.

Based on this catalyst design concept, Fe-, Co-, and Ni-doped zeolite X as high active catalysts were also synthesized and successfully applied for direct oxidative coupling of alkenes with aldehydes to prepare α,β -epoxy ketones, which are crucial intermediates for many natural products and drug molecules. Recently, Liu and co-workers reported that the oxidative coupling of alkenes with aldehydes was catalyzed by iron-salts-furnished β -peroxy ketones that can be transformed further into the corresponding epoxides in the presence of organic bases [41]. More recently, we reported that the α,β -epoxy ketones can be synthesized by the direct oxidative coupling of alkenes with aldehydes over the basic zeolite X and ETS-10 catalysts [42]. In this work, the prepared Fe-, Co-, Ni-, and Cu-doped zeolite X as functional catalysts show more activity than the single basic zeolite X catalyst (Table 8), and the scope of the substrate is listed in Table S3 in the Supplementary Information. The plausible reaction mechanism is shown in Fig. S4 in the Supplementary Information.

4. Conclusions

In summary, considering the characteristics and the mechanism of the decarboxylative coupling of CAs with alcohols and the oxidative coupling of alkenes with aldehydes, metal-doped zeolite-X (Cu-X, Fe-X, Co-X, and Ni-X) catalysts were successfully synthesized. The Cu-X catalyst has extraordinarily high activity in the decarboxylative coupling of CAs with alcohols, alkylbenzenes, cycloalkanes, and cyclic ethers. All the catalysts show superior catalytic performance in the direct oxidative coupling of alkenes with

aldehydes. The catalyst design concept in this work would open a new door for the preparation of highly active heterogeneous catalysts in synthetic chemistry.

Acknowledgments

This work was supported by the National Natural Science Foundation of China (U1463203 and 21476030) and the Natural Science Foundation of Zhejiang Province of China (LZ14B060003).

Appendix A. Supplementary material

Supplementary data associated with this article can be found, in the online version, at <http://dx.doi.org/10.1016/j.jcat.2016.01.030>.

References

- [1] X. Zhang, A. Corma, *Angew. Chem. Int. Ed.* 120 (2008) 4430.
- [2] M.J. Climent, A. Corma, S. Iborra, *Chem. Rev.* 111 (2011) 1072.
- [3] V. Guillerme, Ł.J. Weseliński, Y. Belmabkhout, A.J. Cairns, V. D'Elia, Ł. Wojtas, K. Adil, M. Eddaoudi, *Nat. Chem.* 6 (2014) 673.
- [4] A.H. Chughtai, N. Ahmad, H.A. Younus, A. Laypkovc, F. Verpoort, *Chem. Soc. Rev.* 44 (2015) 6804.
- [5] Á. Molnár, *Chem. Rev.* 111 (2011) 2251.
- [6] J.R. Cabrero-Antonino, A. Leyva-Pérez, A. Corma, *Angew. Chem. Int. Ed.* 127 (2015) 5750.
- [7] C.M. McGuirk, M.J. Katz, C.L. Stren, A.A. Sarjeant, J.T. Hupp, O.K. Farha, C.A. Mirkin, *J. Am. Chem. Soc.* 137 (2015) 91.
- [8] S.-W. Kim, M. Kim, W.Y. Lee, T. Hyeon, *J. Am. Chem. Soc.* 124 (2002) 7642.
- [9] M. Choi, D.-H. Lee, K. Na, B.-W. Yu, R. Ryoo, *Angew. Chem. Int. Ed.* 48 (2009) 3673.
- [10] B. Yuan, Y. Pan, Y. Li, B. Yin, H. Jiang, *Angew. Chem. Int. Ed.* 49 (2010) 4054.
- [11] S.-Y. Ding, J. Gao, Q. Wang, Y. Zhang, W.-G. Song, C.-Y. Su, W. Wang, *J. Am. Chem. Soc.* 133 (2011) 19816.
- [12] A. Stein, B.J. Melde, R.C. Schroden, *Adv. Mater.* 12 (2000) 1403.
- [13] D.E.D. Vos, M. Dams, B.F. Sels, P.A. Jacobs, *Chem. Rev.* 102 (2002) 3615.
- [14] C.M. Crudden, M. Sateesh, R. Lewis, *J. Am. Chem. Soc.* 127 (2005) 10045.
- [15] J.D. Webb, S. MacQuarrie, K. McEleney, C.M. Crudden, *J. Catal.* 252 (2007) 97.
- [16] L. Zhao, Y. Li, P. Yu, X. Han, J. He, *ACS Catal.* 2 (2012) 1118.
- [17] J. Jiang, O.M. Yaghi, *Chem. Rev.* 115 (2015) 6966.
- [18] R.G. Bergman, *Nature* 446 (2007) 391.
- [19] X. Chen, K.M. Engle, D.-H. Wang, J.-Q. Yu, *Angew. Chem. Int. Ed.* 48 (2009) 5094.
- [20] A.F.M. Noisier, M.A. Brimble, *Chem. Rev.* 114 (2014) 8775.
- [21] A. Ford, H. Miel, A. Ring, C.N. Slattery, A.R. Maguire, M.A. McKerverey, *Chem. Rev.* 115 (2015) 9981.
- [22] L. Huang, M. Arndt, K. Gooßen, H. Heydt, L.J. Gooßen, *Chem. Rev.* 115 (2015) 2596.
- [23] H. Yang, P. Sun, Y. Zhu, H. Yan, L. Lu, X. Qu, T. Li, J. Mao, *Chem. Commun.* 48 (2012) 784.
- [24] H. Huang, K. Jia, Y. Chen, *Angew. Chem. Int. Ed.* 54 (2015) 1881.
- [25] J. Ji, P. Liu, P. Sun, *Chem. Commun.* 51 (2015) 7546.
- [26] M.C. Willis, *Chem. Rev.* 110 (2010) 725.
- [27] R.I. McDonald, G. Liu, S.S. Stahl, *Chem. Rev.* 111 (2011) 2981.
- [28] Z. He, T. Luo, M. Hu, Y. Cao, J. Hu, *Angew. Chem. Int. Ed.* 51 (2012) 3944.

- [29] Z. Cui, X. Shang, X.-F. Shao, Z.-Q. Liu, *Chem. Sci.* 3 (2012) 2853.
- [30] R.J. Davis, *J. Catal.* 216 (2003) 396.
- [31] A. Inayat, I. Knoke, E. Spiecker, W. Schwieger, *Angew. Chem. Int. Ed.* 51 (2012) 1962.
- [32] B.L. Su, D. Barthomeuf, *Appl. Catal. A* 124 (1995) 73.
- [33] R.C. Deka, R.K. Roy, K. Hirao, *Chem. Phys. Lett.* 332 (2000) 576.
- [34] D. Barthomeuf, *J. Phys. Chem. B* 109 (2005) 2047.
- [35] W. Fu, T. Liu, Z. Fang, Y. Ma, X. Zheng, W. Wang, X. Ni, M. Hu, T. Tang, *Chem. Commun.* 51 (2015) 5890.
- [36] X. Zhou, H. Chen, X. Cui, Z. Hua, Y. Chen, Y. Zhu, Y. Song, Y. Gong, J. Shi, *Appl. Catal. A* 451 (2013) 112.
- [37] F. Bin, X. Wei, B. Li, K.S. Hui, *Appl. Catal. B* 162 (2015) 282.
- [38] P. Vanelderen, J. Vancauwenbergh, B.F. Sels, R.A. Schoonheydt, *Coord. Chem. Rev.* 257 (2013) 483.
- [39] A. Sultana, T. Nanba, M. Haneda, M. Sasaki, H. Hamada, *Appl. Catal. B* 101 (2010) 61.
- [40] M. Huang, S. Kaliaguin, *J. Chem. Soc., Faraday Trans.* 88 (1992) 751.
- [41] W. Liu, Y. Li, K. Liu, Z. Li, *J. Am. Chem. Soc.* 133 (2011) 10756.
- [42] M. Xiang, X. Ni, X. Yi, A. Zheng, W. Wang, M. He, J. Xiong, T. Liu, Y. Ma, P. Zhu, X. Zheng, T. Tang, *ChemCatChem* 7 (2015) 521.